



Impact of nanoparticles mixtures on mineral and pongamia ester oils dielectric strength

M. Yamuna¹ · R. Madavan¹

Received: 27 July 2022 / Revised: 16 August 2022 / Accepted: 17 August 2022 / Published online: 1 September 2022
© The Author(s), under exclusive licence to Springer-Verlag GmbH Germany, part of Springer Nature 2022

Abstract

The heart of an electrical system network is power transformers, and its livelihood is insulating oil, which provides insulation and cooling to the transformers. The elements of insulating oil determine the electrical properties of the oil, and the properties of the insulating oil can be optimized by bring in nanofluid. The chief aim of this work is to analyze the impact of Fe_3O_4 , ZnO and TiO_2 nanoparticles individually and its mixtures ($\text{Fe}_3\text{O}_4 + \text{ZnO}$) and ($\text{Fe}_3\text{O}_4 + \text{TiO}_2$) at different volume concentration on dielectric strength of mineral oil and ester oil. Laboratory-oriented experimental results are statistically analyzed using normal and Weibull distribution technique. The results of the experiments reveal that conductive nanoparticles blended mineral oil and pongamia ester oil-based nanofluids samples S6 (MO + 0.4% Fe_3O_4) and S18 (EO + 0.4% Fe_3O_4) reported with highest enhancement percentage in BDV as 52% and 53%, respectively, compared to other nanoparticles. While looking over the performance of mixed nanoparticles, the samples (S27 MO + 75% Fe_3O_4 + 25% TiO_2) and S33 (EO + 75% Fe_3O_4 + 25% TiO_2) reported with highest enhancement percentage in Breakdown Voltage (BDV) as 65% and 69%, respectively. When comparing the BDV of individual nanofluid samples and mixed nanofluid samples, the mixed nanofluid samples have higher enhancement percentage.

Keywords Pongamia ester oil · Nanofluids · Mixed nanofluids · Breakdown voltage · Weibull analysis

1 Introduction

Most commonly utilized insulating liquid in oil-filled devices such as power transformers, tap changers, power capacitors, bushings, circuit breakers and cables is Mineral oil (MO). It has strong dielectric strength and thermal performance, which are two important qualities for this type of component [1]. There are many different types of transformer fluids available nowadays, but ecologically friendly liquids are the most recent breakthrough in dielectric fluids for electrical transformers, bushings, circuit breakers and others. These fluids, also known as natural esters or bio-based fluids, are produced spontaneously by living organisms and are derived from plant crops such as coconut, neem, palm, rapeseed, sunflower, and others. Because of its environmentally friendly characteristics and strong fire

resistance, this novel "green" alternative has found a niche in the market [2–4].

Dielectric properties, heat transfer ability and physical properties are the important qualities of transformer fluid. It can be further enhanced by using specialized nanoparticles (NP), such as conductive and semi-conductive. Indeed, the resulting nanofluids (NF) have higher thermal characteristics [5] as well as dielectric and physical properties than MO and ester oil. Choi and Eastern developed the concept of NF in 1995 [6] and detailed its advantages over traditional fluids for cooling and systems in various engineering applications[7]. Water, deionized water, glycol/water solutions, fluorocarbons, hydrogenated poly-alpha-olefins were utilized as base fluids for heat transfer fluid. Solar absorption, nuclear power plants, transportation, civil engineering, aircrafts, space stations and other applications of NF come to mind. The volume fraction, shape, sizes, and qualities of the NP added, as well as the surface contact area between particles and liquid, all influence the cooling effectiveness of NF [8–10].

It was reported that by adding particular type of nanoparticles in mineral oil- and ester oil-based nanofluids can

✉ R. Madavan
srmadavan@gmail.com

¹ Department of Electrical and Electronics Engineering, PSR Engineering College, Sivakasi, India 626140

Table 1 Basic properties of Mineral oil and Pongamia Ester oil

Parameter	Mineral Oil	Pongamia Ester Oil
Dielectric Strength (kV)	41.2	62.7
Flash point (°C)	135	314
Fire point (°C)	147	328
Pour point (°C)	-48	-26
Acidity (mg KOH/g)	0.0015	0.0048
Water content (ppm)	8.2	32
Dissipation factor at 90 °C	0.0071	0.063

considerably increase their dielectric, thermal, and physical properties [11, 12]. In the previous two decades, numerous studies have been undertaken on this subject. Aluminum oxide (Al_2O_3), aluminum (Al), copper (Cu), copper oxide (CuO), titanium dioxide (TiO_2), iron oxide (Fe_3O_4), zinc oxide (ZnO), silicon dioxide (SiO), fullerene (C_{60}), carbon nanotubes (CNT) and calcium copper titanate (CCTO) are the most commonly studied NPs. According to the studies published in the literature, Fe_3O_4 NPs improve the properties

of MO as well as ester oil the most. These advances in dielectric and thermal qualities enable transformer size, weight, and cost reductions, as well as the transmission of significantly higher power densities [8–13].

The findings reported are focused on analyzing the impact of each type of NP employed separately. The aim of this work is to analyze the impact of varying concentrations of Fe_3O_4 , TiO_2 and ZnO nanoparticles on the dielectric strength of mineral oil and pongamia ester oil (EO). Further, the results are examined using statistical analysis.

2 Samples preparation

The liquid insulation utilized in this work is mineral oil and pongamia ester oil. Initially, the oils should be pretreated to remove foreign particles and moisture content which affects the performance of liquid insulation. In the pretreatment process, the oils are heated up to 100 °C to remove moisture content and filtered with Whatman filter paper to remove foreign particles. After the pretreatment process, moisture content in mineral oil and pongamia ester oil is 5.2 ppm and

Fig. 1 SEM images of (a) Fe_3O_4 , (b) ZnO and (c) TiO_2

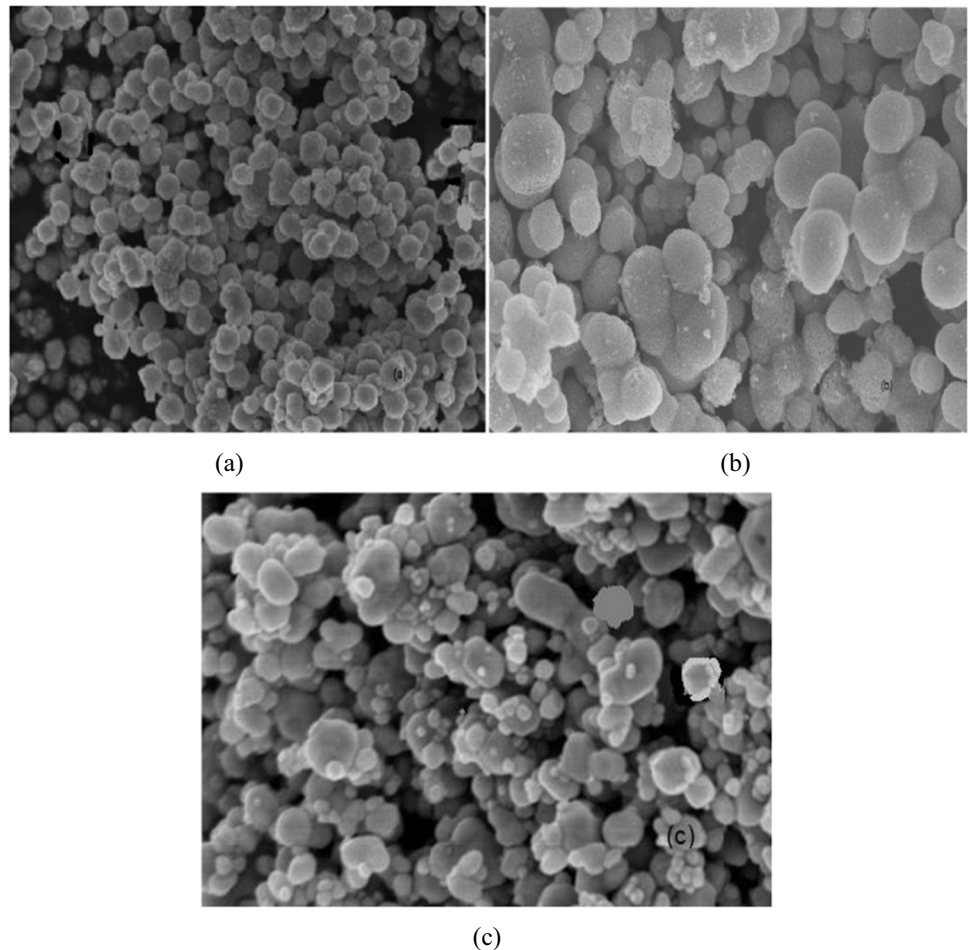
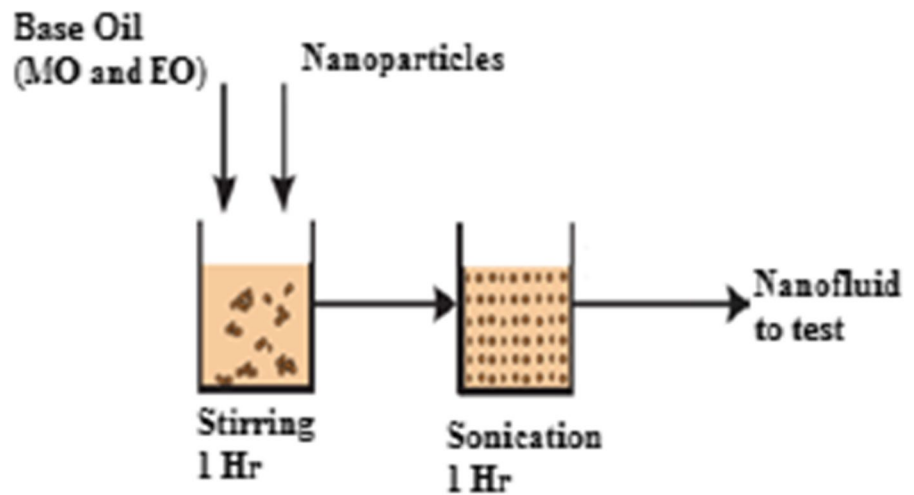


Fig. 2 Nanofluid preparation process



18.6 ppm, respectively. The base properties of mineral oil and pongamia ester oil are given in Table 1.

In this work, three nanoparticles namely Fe_3O_4 , ZnO and TiO_2 are used for analysis purpose. The shape of the nanoparticles is in spherical as shown in Fig. 1, SEM images of nanoparticles. Similarly, the size distribution of the nanoparticles is less than 70 nm. With these nanoparticles, two different sets of mineral oil and pongamia ester oil based nanofluids samples are prepared for laboratory oriented experiments. During the nanofluids preparation process, the samples are placed in magnetic stirring process for 1 h. Further, the samples undergo ultra-sonication process for 1 h to avoid agglomeration of nanoparticles and to have uniform and stable blending of nanoparticles as shown in Fig. 2. In the first set, Fe_3O_4 , ZnO and TiO_2 nanoparticles individually blended with mineral oil and pongamia ester oil at 0.1%, 0.2%, 0.3% and 0.4% volume concentration. Subsequently, in the second set, mixtures of Fe_3O_4 , and TiO_2 nanoparticles

and mixtures of Fe_3O_4 , and ZnO nanoparticles are blended with mineral oil and pongamia ester oil. The detailed samples list is given in Table 2, and some of the samples are shown in Fig. 3.

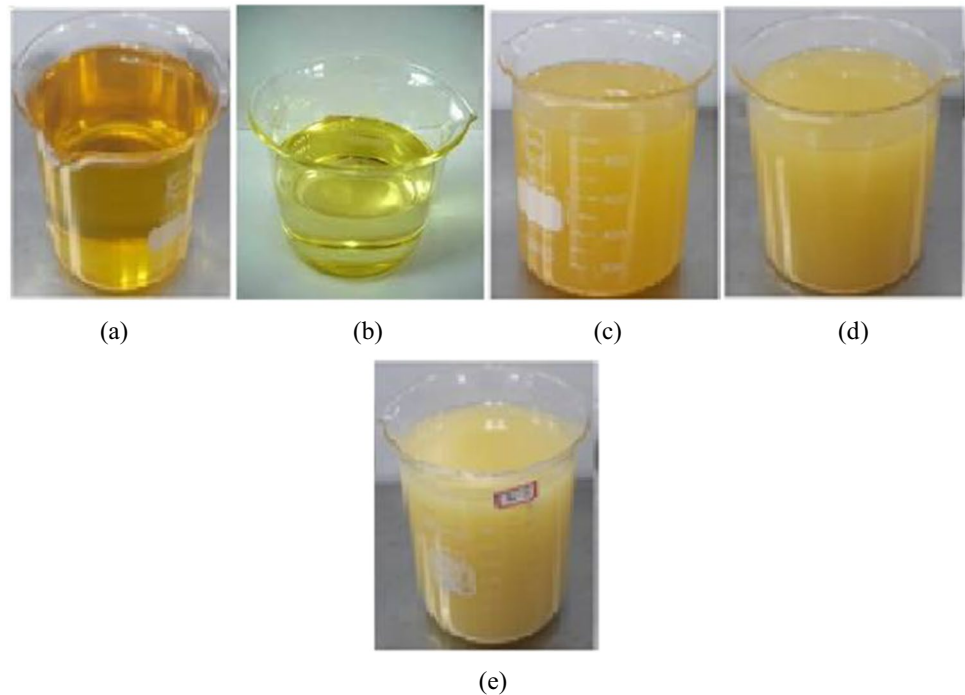
3 Experimental results

The BDV test is an important aspect of the liquid insulation acceptance testing. With the spacing of 2.5 mm, two copper plate electrodes are used for BDV test as shown in Fig. 4. In order to generate high AC voltage, the samples are electrically strained using step up transformer. The BDV tests are conducted with the same electrodes as the ac breakdown experiments. All the BDV tests are carried out in the same temperature range as a thermal test in an incubator to study the effect of temperature on breakdown behavior [14]. For the purpose of decreasing the influence of production and growth

Table 2 Samples preparation description

S.No	Sample Description	S.No	Sample Description	S.No	Sample Description
S1	Pure mineral oil	S15	EO + 0.1% Fe_3O_4	S27	MO + 75% Fe_3O_4 + 25% TiO_2
S2	Pure pongamia ester oil	S16	EO + 0.2% Fe_3O_4	S28	MO + 50% Fe_3O_4 + 50% TiO_2
S3	MO + 0.1% Fe_3O_4	S17	EO + 0.3% Fe_3O_4	S29	MO + 25% Fe_3O_4 + 75% TiO_2
S4	MO + 0.2% Fe_3O_4	S18	EO + 0.4% Fe_3O_4	S30	MO + 75% Fe_3O_4 + 25% ZnO
S5	MO + 0.3% Fe_3O_4	S19	EO + 0.1% TiO_2	S31	MO + 50% Fe_3O_4 + 50% ZnO
S6	MO + 0.4% Fe_3O_4	S20	EO + 0.2% TiO_2	S32	MO + 25% Fe_3O_4 + 75% ZnO
S7	MO + 0.1% TiO_2	S21	EO + 0.3% TiO_2	S33	EO + 75% Fe_3O_4 + 25% TiO_2
S8	MO + 0.2% TiO_2	S22	EO + 0.4% TiO_2	S34	EO + 50% Fe_3O_4 + 50% TiO_2
S9	MO + 0.3% TiO_2	S23	EO + 0.1% ZnO	S35	EO + 25% Fe_3O_4 + 75% TiO_2
S10	MO + 0.4% TiO_2	S24	EO + 0.2% ZnO	S36	EO + 75% Fe_3O_4 + 25% ZnO
S11	MO + 0.1% ZnO	S25	EO + 0.3% ZnO	S37	EO + 50% Fe_3O_4 + 50% ZnO
S12	MO + 0.2% ZnO	S26	EO + 0.4% ZnO	S38	EO + 25% Fe_3O_4 + 75% ZnO
S13	MO + 0.3% ZnO	-	-	-	-
S14	MO + 0.4% ZnO	-	-	-	-

Fig. 3 (a) Pure MO, (b) Pure EO, (c) MO+0.4% Fe₃O₄, (d) EO+0.4% Fe₃O₄, (e) EO+25% Fe₃O₄+75% TiO₂



of vapor bubbles, the highest temperature is limited to 70 °C, which is less than the boiling point of liquid samples.

The average BDV of pure MO, pure EO and nanofluid samples is shown in Table 3. It is inferred that nanofluid samples have higher average BDV than average BDV of pure MO and EO samples. In particular, Fe₃O₄-blended nanofluid samples (both MO- and EO-based nanofluids) have higher average BDV than TiO₂- and ZnO-blended nanofluid samples. The Fe₃O₄ nanofluid sample with 0.4% concentration in both MO and EO (i.e., sample number S6 and S18)

registered best average BDV as 62.8 kV for MO and 91.5 kV for EO compared to other nanofluid samples as shown in Figs. 5 and 6. Moreover, when comparing the enhancement percentage of nanofluid samples BDV, Fe₃O₄-blended nanofluid samples (both MO and EO) performed better and have higher enhancement percentage than TiO₂- and ZnO-blended nanofluid samples. In particular, nanofluid sample with 0.4% Fe₃O₄ concentration registered highest enhancement percentage as 52% for MO (sample S6) and 53% for EO (sample S18) than other nanofluid samples.

Fig. 4 BDV test setup

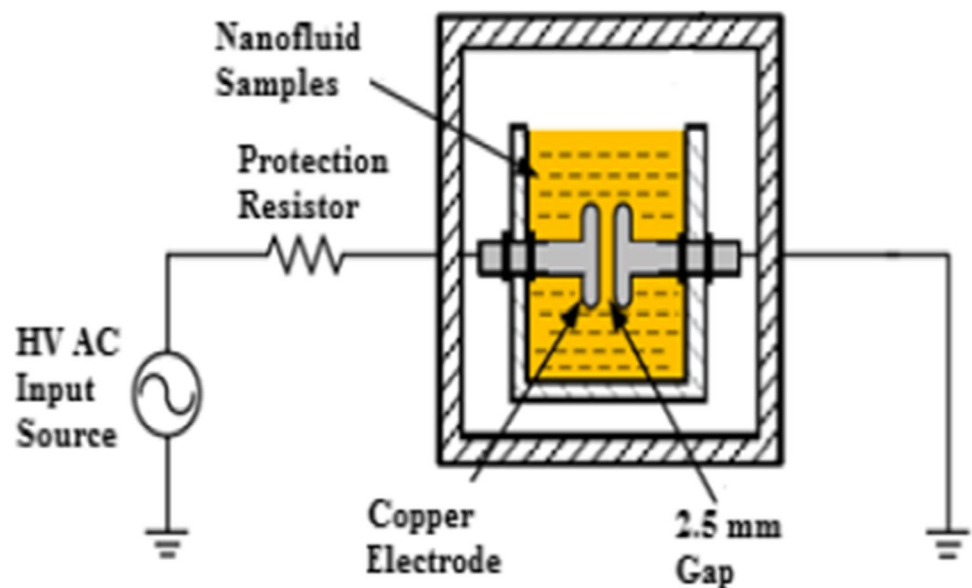


Table 3 Average BDV of nanofluid samples

Sample Number	Dielectric Strength (kV)	Enhancement in Dielectric Strength (%)	Sample Number	Dielectric Strength (kV)	Enhancement in Dielectric Strength (%)
S1	41.2	-	S15	80.9	38
S2	58.7	-	S16	82.6	41
S3	52.5	27	S17	85.4	45
S4	54.2	32	S18	91.5	53
S5	57.4	39	S19	79.6	36
S6	62.8	52	S20	82.1	40
S7	50.6	23	S21	86.4	47
S8	53.4	30	S22	85.5	46
S9	55.3	34	S23	81.4	36
S10	54.2	32	S24	80.3	37
S11	50.4	22	S25	82.6	39
S12	51.8	26	S26	84.5	44
S13	53.5	30	-	-	-
S14	52.4	27	-	-	-

Fig. 5 Average Breakdown Voltage of MO-based nanofluid Samples

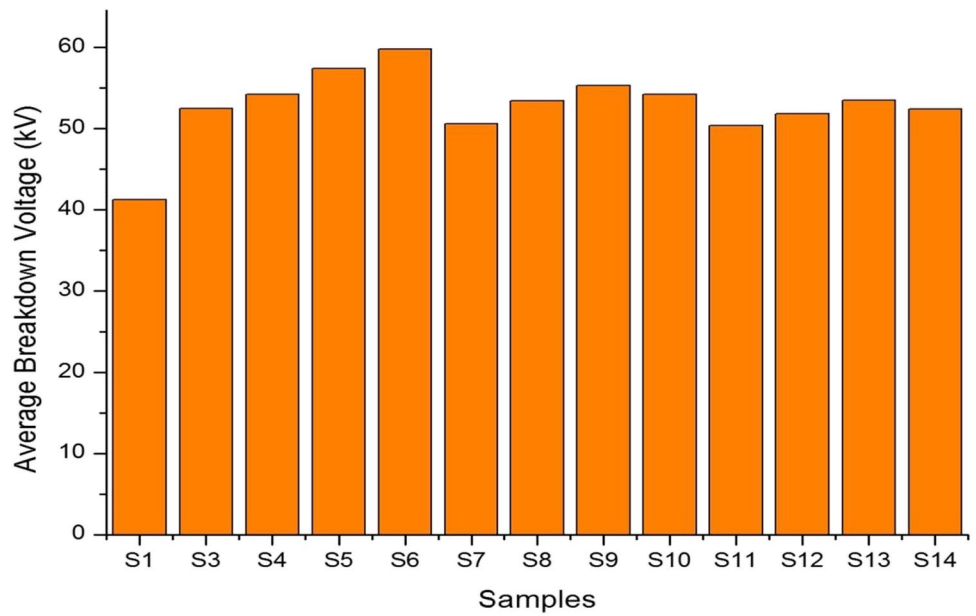


Fig. 6 Average Breakdown Voltage of EO-based nanofluid Samples

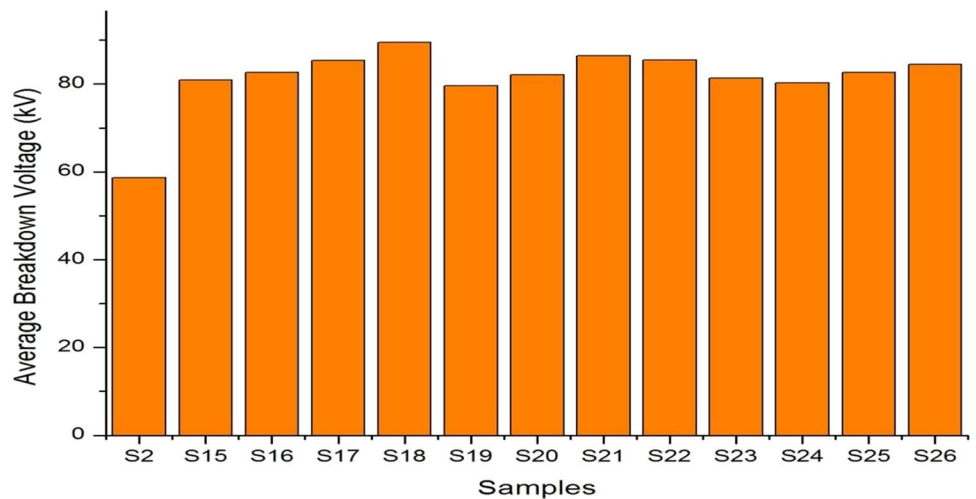
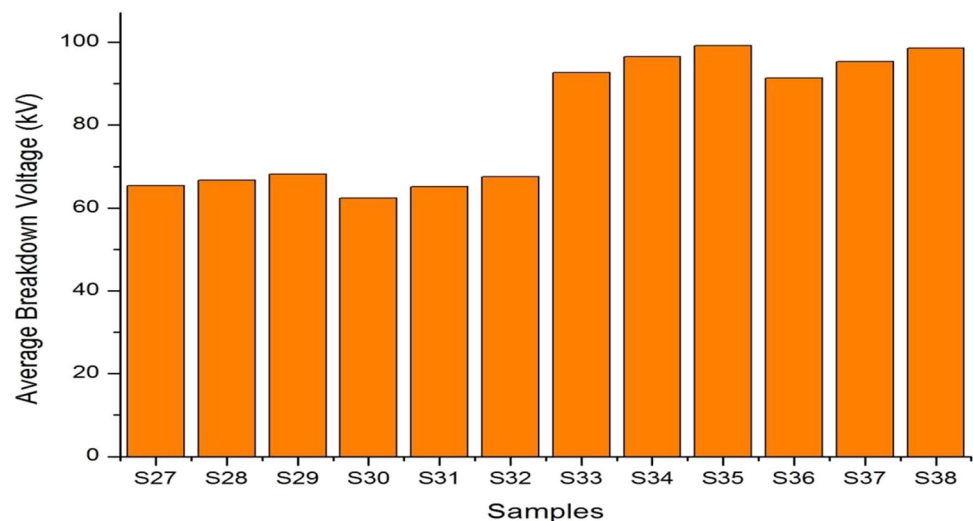


Table 4 Average BDV of mixtures of nanofluid samples

Sample Number	Dielectric Strength (kV)	Enhancement in Dielectric Strength (%)
S27	68.1	65
S28	66.7	62
S29	65.4	59
S30	62.4	51
S31	65.2	58
S32	67.5	64
S33	99.2	69
S34	96.5	64
S35	92.7	58
S36	91.4	56
S37	95.3	62
S38	98.6	68

The effect of blending mixtures of nanoparticles in MO and EO on average BDV is shown in Table 4. The nanoparticles mixtures are prepared by addition of two nanoparticles such as $\text{Fe}_3\text{O}_4 + \text{ZnO}$ and $\text{Fe}_3\text{O}_4 + \text{TiO}_2$ nanoparticles at various ratios as given in Table 2. The experimental results of mixtures of nanoparticles on MO and EO are given in Table 4 and for better understating it are shown in Fig. 7. It is noted that in all concentrations, nanoparticles mixtures enhance the BDV of MO and EO than nanoparticle samples as individually (i.e., S3 to S14 for MO and S15 to S26 for EO). Moreover, the mixture samples S27 (MO + 75% Fe_3O_4 + 25% TiO_2) and S33 (EO + 75% Fe_3O_4 + 25% TiO_2) performed better and produce some appreciable improvement in average BDV 68.1 kV and 99.2 kV, respectively. Moreover, samples S29 and S35 recorded highest enhancement percentage as 65% and 69%, respectively.

Fig. 7 Average Breakdown Voltage of mixed nanofluid Samples

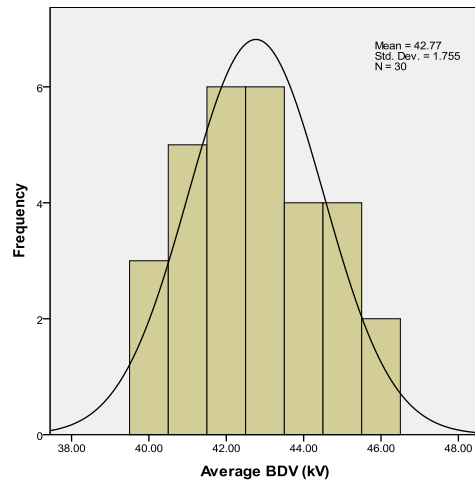
4 Statistical analysis

The widely used statistical techniques to analyze experimental results of liquid dielectrics breakdown voltage are Weibull and normal distribution. In order to verify the distribution level of experimental results, hypothesis test will be carrying out. As a result, we determine the p value, which is a probability that evaluates the proof in favor of the null hypothesis. Stronger evidence is presented in contrast to the null hypothesis by lower p values [15].

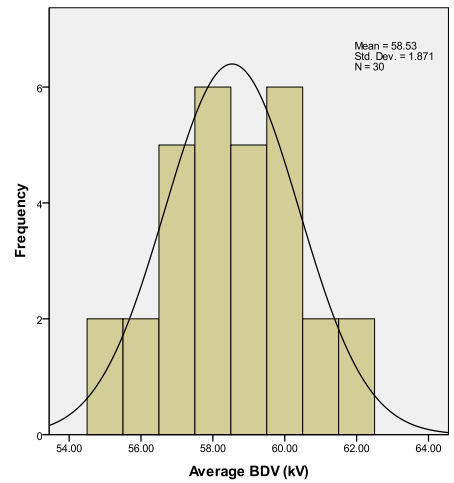
When the p value and significance level are compared, it is possible to assess whether or not the data have a normal distribution. A significance threshold of 0.05 usually produces good results. If the significance threshold is set at 0.05, there is a 5% chance that the results will be interpreted as not following a normal distribution. The choice is to reject null hypothesis and come to the conclusion that the data do not reflect a normal distribution if the p value is below or equal to the probability value. Furthermore, if the p value exceeds the import level, the null hypothesis is not rejected since there is insufficient evidence to support the conclusion that the data do not obey a normal distribution. The data do not, however, necessarily follow the normal distribution; therefore, this cannot be said. The outcomes of the hypothesis test are additionally supported by additional standards, including those imposed by the Jarque–Bera and Pearson, Lillie tests [16].

The histogram distribution of BDV of examined nanofluids samples is shown in Fig. 8. This permits us to observe the abnormalities in the distribution of BDV in various ranges of voltages. It is inferred that with the irregularities in BDV of nanofluid samples S5 (MO + 0.3% Fe_3O_4), S10 (MO + 0.4% TiO_2), S13 (MO + 0.3% ZnO), S17 (EO + 0.3% Fe_3O_4), S21 (EO + 0.3% TiO_2), S26 (EO + 0.4% ZnO), S30 (MO + 75% Fe_3O_4 + 25% ZnO) and S36 (EO + 75% Fe_3O_4 + 25% ZnO) are having lower p value. In addition, the experimental data

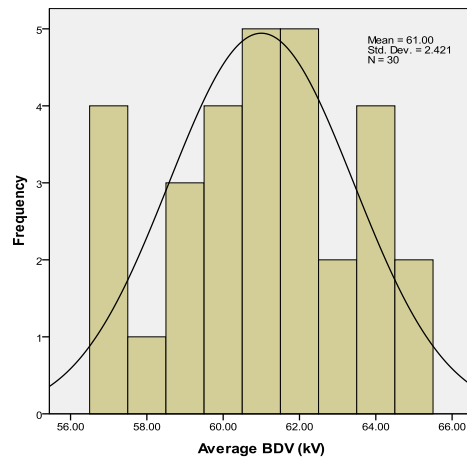
Fig.8 Histogram distribution of nanofluids



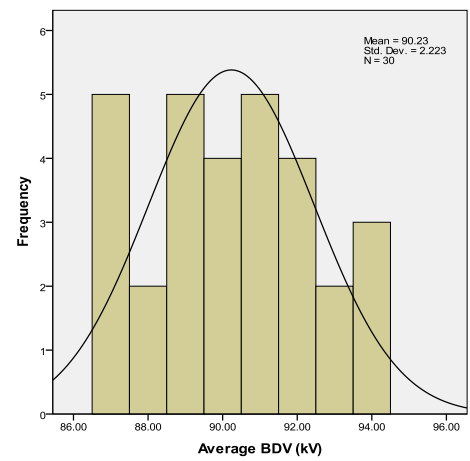
(a) Pure MO



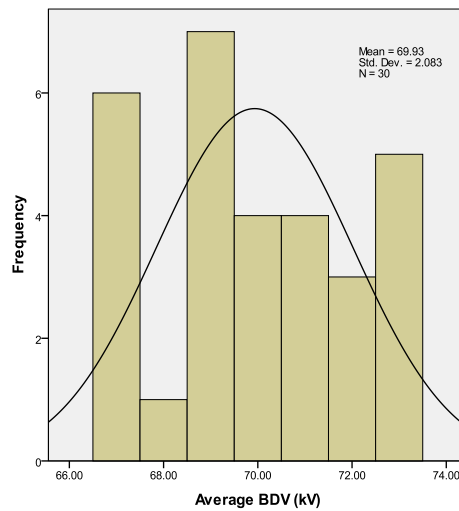
(b) Pure EO



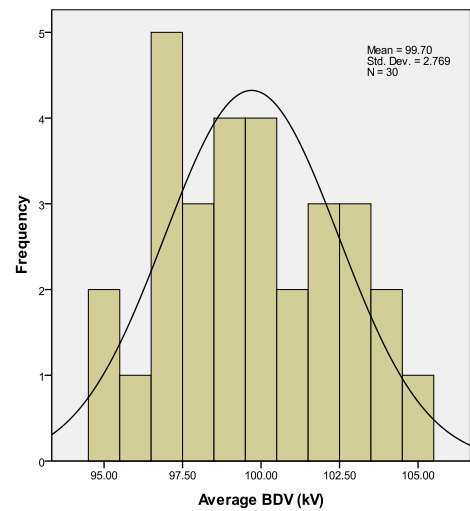
(c) MO + 0.4% Fe₃O₄



(d) EO + 0.4% Fe₃O₄



(e) MO+75% Fe₃O₄+25% TiO₂



(f) EO+75% Fe₃O₄+25% TiO₂

of examined nanofluid samples follow the normal distribution as shown in Table 5.

The measures of skewness and kurtosis are also used to determine whether there is any issue with non-normality. Skewness is a metric for symmetry or, more specifically,

for the absence of symmetry. An experimental data set is said to be symmetric if it has the same appearance to the right and left of the center point. Kurtosis measures a distribution's peakedness and the degree to which the data are heavily or lightly tailed in relation to a normal distribution.

Table 5 Nanofluids BDV conformity test

Sample Number	Normal Distribution		Weibull Distribution	
	<i>p</i> -value	Remarks	<i>p</i> -value	Remarks
S1	0.2264	Accepted	0.2117	Accepted
S2	0.2345	Accepted	0.2524	Accepted
MO-based nanofluids				
S3	0.4514	Accepted	0.5423	Accepted
S4	0.3761	Accepted	0.3416	Accepted
S5	0.0062	Not Accepted	0.0101	Not Accepted
S6	0.5672	Accepted	0.5945	Accepted
S7	0.3247	Accepted	0.4318	Accepted
S8	0.4271	Accepted	0.5872	Accepted
S9	0.5624	Accepted	0.4675	Accepted
S10	0.0112	Not Accepted	0.0045	Not Accepted
S11	0.4376	Accepted	0.3783	Accepted
S12	0.3462	Accepted	0.4862	Accepted
S13	0.0023	Not Accepted	0.0016	Not Accepted
S14	0.4768	Accepted	0.5724	Accepted
EO-based nanofluids				
S15	0.5347	Accepted	0.5846	Accepted
S16	0.4521	Accepted	0.5024	Accepted
S17	0.3758	Accepted	0.4287	Accepted
S18	0.0036	Not Accepted	0.0027	Not Accepted
S19	0.4892	Accepted	0.4562	Accepted
S20	0.5645	Accepted	0.5143	Accepted
S21	0.0102	Not Accepted	0.0067	Not Accepted
S22	0.4652	Accepted	0.5217	Accepted
S23	0.5743	Accepted	0.5973	Accepted
S24	0.4276	Accepted	0.4831	Accepted
S25	0.2985	Accepted	0.3786	Accepted
S26	0.0032	Not Accepted	0.0021	Not Accepted
Mixed nanofluids				
S27	0.5627	Accepted	0.5214	Accepted
S28	0.4726	Accepted	0.4127	Accepted
S29	0.3875	Accepted	0.3262	Accepted
S30	0.0110	Not Accepted	0.0027	Not Accepted
S31	0.4382	Accepted	0.5752	Accepted
S32	0.5972	Accepted	0.4975	Accepted
S33	0.3478	Accepted	0.3872	Accepted
S34	0.4572	Accepted	0.5014	Accepted
S35	0.5624	Accepted	0.5967	Accepted
S36	0.0109	Not Accepted	0.0041	Not Accepted
S37	0.3219	Accepted	0.4215	Accepted
S38	0.4837	Accepted	0.5621	Accepted

In other words, data sets with a higher kurtosis have heavier tails. Low kurtosis data typically have lighter tails. Some researchers reported that the asymmetry and kurtosis values between -2 and +2 are considered to prove the distribution is normal [16].

Tables 6, 7 and 8 show the Skewness and kurtosis values of examined nanofluids. Except the nanofluid sample S30 (MO + 75% Fe₃O₄ + 25% ZnO), skewness and kurtosis are higher than 3, and the kurtosis value of samples S5 (MO + 0.3% Fe₃O₄), S10 (MO + 0.4% TiO₂), S13 (MO + 0.3% ZnO), S17 (EO + 0.3% Fe₃O₄), S21 (EO + 0.3% TiO₂), S26 (EO + 0.4% ZnO) and S36 (EO + 75% Fe₃O₄ + 25% ZnO) is between 2 and 3. Remaining all other nanofluid samples, the skewness and kurtosis values are lesser than 2. Nevertheless, the higher kurtosis value 3 does not eliminate the data of normality. In fact, most statistical software programmes, including SPSS [16], offer “extra” kurtosis that is determined via subtracting 3 from the kurtosis for various practical purposes.

For a fully normal distribution, the extra kurtosis ought to be zero. The samples S30 (MO + 25% Fe₃O₄ + 25% ZnO) sample out of all the examined nanofluid samples has a kurtosis value of 3.19176, giving it an extra of 0.19176. This an extra is not that significant when taking into account data that deviate from normality. Leptokurtic distributions, which have a high peak, are defined as having a positive extra kurtosis, while Platykurtic distributions, which have a negative extra kurtosis, are defined as having a flat-topped curve. In light of the foregoing, it can be said that all samples follow the normal distribution. Based on the p value, the samples S5 (MO + 0.3% Fe₃O₄), S10 (MO + 0.4% TiO₂), S13 (MO + 0.3% ZnO), S17 (EO + 0.3% Fe₃O₄), S21 (EO + 0.3% TiO₂), S26 (EO + 0.4% ZnO), S30 (MO + 75% Fe₃O₄ + 25% ZnO) and S36 (EO + 75% Fe₃O₄ + 25% ZnO) do not follow normal distribution.

Table 6 Skewness and kurtosis of BDV of MO-based nanofluids

Sample No.	skewness	kurtosis
S1	0.17715	-0.86296
S3	-0.00863	-0.82358
S4	0.05056	-0.92204
S5	-0.06120	2.69854
S6	0.07178	-0.94982
S7	-0.14057	-0.83144
S8	-0.33384	-0.51666
S9	0.06581	-0.23067
S10	0.06746	2.29289
S11	-0.42273	0.06670
S12	-0.33063	-0.82303
S13	-0.46322	2.45161
S14	0.08013	-0.25017

Table 7 Skewness and kurtosis of BDV of MO-based nanofluids

Sample No.	skewness	kurtosis
S2	-0.03894	-0.51979
S15	0.13681	-0.24652
S16	-0.27733	-0.41024
S17	0.08827	2.96021
S18	-0.30915	0.74328
S19	-0.35532	-0.46754
S20	-0.18143	-1.20364
S21	0.14904	2.59733
S22	-0.40080	-0.69545
S23	0.36141	-0.53479
S24	-0.29912	-0.68196
S25	0.37135	-0.18999
S26	-0.24103	2.77773

Weibull probability plots for dielectric strength of mineral and pongamia ester oil-based Fe₃O₄, TiO₂ and ZnO nanofluids for different volume concentrations of nanoparticles are shown in Fig. 9. The scale parameter is connected to data dispersion and reflects the degree of failure. The shape parameter is equal to the line's slope. The probabilities for the different examined nanofluid samples are listed in Table 5 along with their conformity to the normal and Weibull distribution. It is observed from the calculated p value, for experimental data of dielectric strength for most of the nanofluids samples are higher when compared to the significance value. Moreover, the BDV of samples S5 (MO + 0.3% Fe₃O₄), S10 (MO + 0.4% TiO₂), S13 (MO + 0.3% ZnO), S17 (EO + 0.3% Fe₃O₄), S21 (EO + 0.3% TiO₂), S26 (EO + 0.4% ZnO), S30 (MO + 75% Fe₃O₄ + 25% ZnO) and S36 (EO + 75% Fe₃O₄ + 25% ZnO) are lesser than the significance value. It confirms that the experimental data comply with normal and Weibull distributions. As

Table 8 Skewness and kurtosis of BDV of mixed nanofluids

Sample No.	skewness	Kurtosis
S27	0.75454	0.44030
S28	-0.06120	-0.69854
S29	-0.18291	0.15397
S30	0.33312	3.19176
S31	0.16927	-0.64146
S32	-0.10585	-0.98147
S33	-0.12317	-0.75165
S34	0.07334	-0.79409
S35	0.14602	-0.90205
S36	-0.56149	2.05048
S37	-0.71312	-0.38051
S38	-0.26227	-0.76696

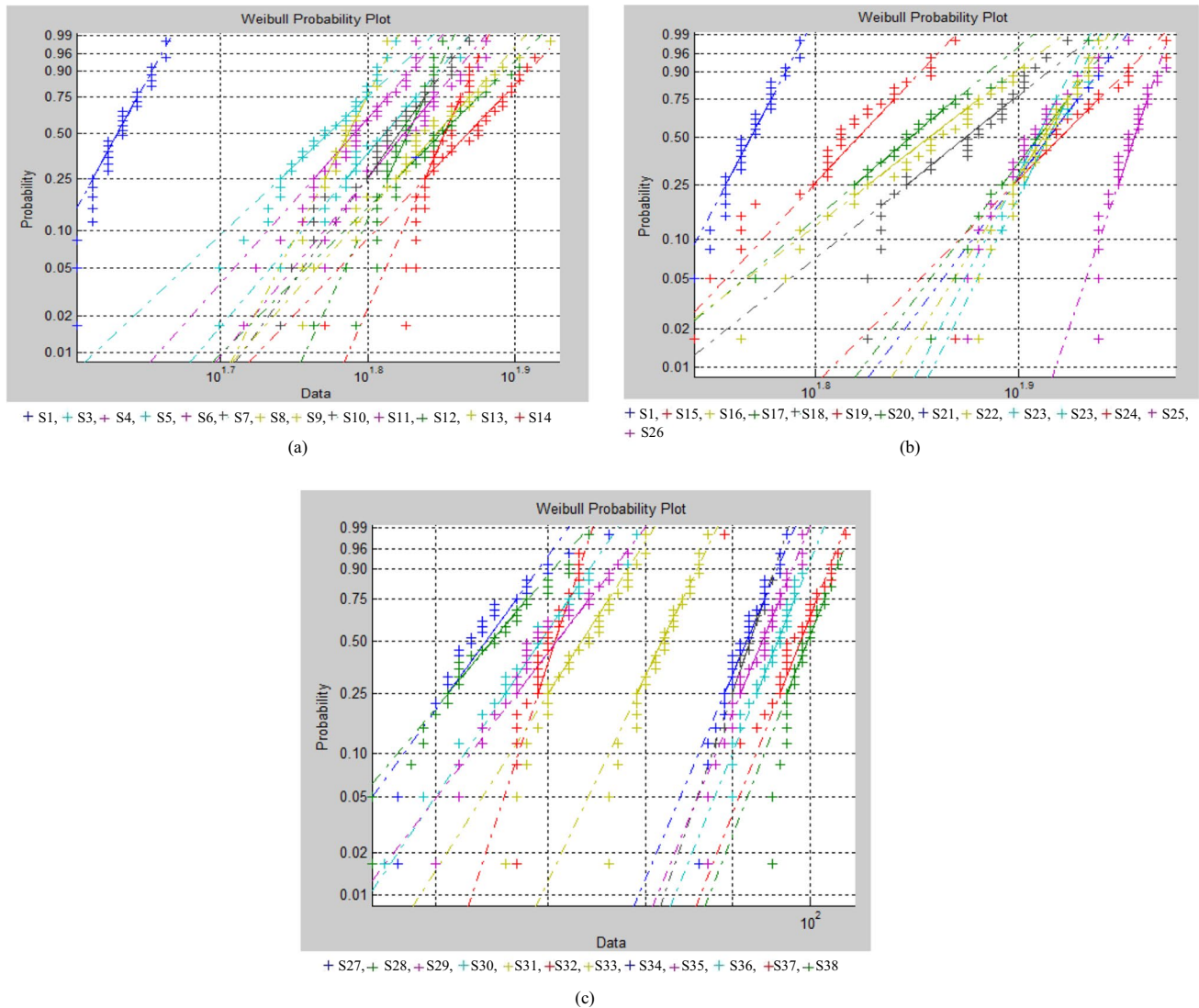


Fig.9 Weibull plot for nanofluids (a) MO, (b) EO and (c) mixed nanofluids

mentioned in the results, experimental data for sphere gap electrode perfectly fit the normal and Weibull distribution.

Table 9 depicts the possible breakdown voltages at 10%, 25% and 50% of examined nanofluids, and this supports to determine voltage limitation for continuous reliable operation of transformers. The BDV at 10% is an approximate possible lowest breakdown voltage. Moreover, it evidences the reliable performance of liquid insulation and it enables the determination of a safety coefficient of electrical equipments. Commonly, the BDV of nanofluid samples is higher than that of pure MO and EO for all three types of nanoparticles and its blending concentrations. For MO and EO, the BDV at 0.4% concentration (samples S6, S10, S14, S17, S22 and S26) of Fe_3O_4 , ZnO and TiO_2 nanoparticles is higher than other concentrations. Similarly, for mixed nanofluids, the concentration at 75% Fe_3O_4 + 25% TiO_2 (sample

S27) and 75% Fe_3O_4 + 25% ZnO (sample S33) has higher BDV than other concentrations. This clearly shows that the blending of nanoparticles enhances the BDV of both MO and EO.

5 Discussion

For the majority of the examined nanofluid samples, the statistical analysis of BDV of experimental data follows both the normal and Weibull distributions. The experimented BDV values of MO- and EO-based nanofluids as well as mixed nanofluids combinations often follow normal rather than Weibull distribution according to the experimental data presented in above section.

Table 9 Nanofluids BDV at different breakdown probabilities

S.No	Sample concentration	10%		25%		50%	
		BDV (kV)	Increment (%)	BDV (kV)	Increment (%)	BDV (kV)	Increment (%)
S1	Pure mineral oil	41.78	-	43.46	-	46.24	-
S2	Pure pongamia ester oil	52.67	-	53.32	-	57.42	-
S3	MO+0.1% Fe ₃ O ₄	42.27	1.17	45.36	4.37	48.45	4.78
S4	MO+0.2% Fe ₃ O ₄	45.32	8.47	48.75	12.17	52.25	13.00
S5	MO+0.3% Fe ₃ O ₄	49.16	17.66	52.34	20.43	57.82	25.04
S6	MO+0.4% Fe ₃ O ₄	52.76	26.28	57.76	32.90	60.34	30.49
S7	MO+0.1% TiO ₂	43.52	4.16	44.83	3.15	47.76	3.29
S8	MO+0.2% TiO ₂	45.78	9.57	46.35	6.65	48.37	4.61
S9	MO+0.3% TiO ₂	47.40	13.45	49.04	12.84	51.78	11.98
S10	MO+0.4% TiO ₂	49.05	17.40	52.17	20.04	55.89	20.87
S11	MO+0.1% ZnO	42.76	2.35	44.85	3.20	48.42	4.71
S12	MO+0.2% ZnO	44.11	5.58	47.53	9.36	50.65	9.54
S13	MO+0.3% ZnO	46.34	10.91	49.72	14.40	53.24	15.14
S14	MO+0.4% ZnO	49.47	18.41	53.09	22.16	57.18	23.66
S15	EO+0.1% Fe ₃ O ₄	64.76	22.95	66.25	24.25	72.00	25.39
S16	EO+0.2% Fe ₃ O ₄	67.52	28.19	68.84	29.11	76.54	33.30
S17	EO+0.3% Fe ₃ O ₄	70.87	34.55	72.49	35.95	81.07	41.18
S18	EO+0.4% Fe ₃ O ₄	75.24	42.85	77.91	46.12	90.23	57.15
S19	EO+0.1% TiO ₂	62.40	18.47	64.71	21.36	70.50	22.78
S20	EO+0.2% TiO ₂	65.71	24.76	68.43	28.34	74.83	30.33
S21	EO+0.3% TiO ₂	71.54	35.83	73.67	38.17	81.47	41.88
S22	EO+0.4% TiO ₂	74.79	42.00	76.42	43.32	83.42	45.28
S23	EO+0.1% ZnO	60.94	15.70	63.04	18.23	68.42	19.16
S24	EO+0.2% ZnO	63.27	20.13	68.15	27.81	75.27	31.09
S25	EO+0.3% ZnO	67.28	27.74	72.76	36.46	79.85	39.06
S26	EO+0.4% ZnO	71.60	35.94	78.62	47.45	86.61	50.84
S27	MO+75% Fe ₃ O ₄ +25% TiO ₂	68.22	63.28	71.37	64.22	76.41	65.25
S28	MO+50% Fe ₃ O ₄ +50% TiO ₂	57.85	38.46	60.72	39.71	64.77	40.07
S29	MO+25% Fe ₃ O ₄ +75% TiO ₂	60.12	43.90	63.75	46.69	68.77	48.72
S30	MO+75% Fe ₃ O ₄ +25% ZnO	63.28	51.46	66.04	51.96	70.60	52.68
S31	MO+50% Fe ₃ O ₄ +50% ZnO	65.34	56.39	68.11	56.72	72.89	57.63
S32	MO+25% Fe ₃ O ₄ +75% ZnO	55.87	33.72	58.24	34.01	63.77	37.90
S33	EO+75% Fe ₃ O ₄ +25% TiO ₂	82.27	56.20	86.47	62.17	95.03	65.50
S34	EO+50% Fe ₃ O ₄ +50% TiO ₂	83.46	58.46	86.29	61.83	93.48	62.80
S35	EO+25% Fe ₃ O ₄ +75% TiO ₂	87.18	65.52	90.73	70.16	99.70	73.63
S36	EO+75% Fe ₃ O ₄ +25% ZnO	80.79	53.39	84.42	58.33	91.77	59.82
S37	EO+50% Fe ₃ O ₄ +50% ZnO	86.45	64.14	88.79	66.52	97.27	69.40
S38	EO+25% Fe ₃ O ₄ +75% ZnO	88.48	67.99	90.48	69.69	98.42	71.40

The experimental results depict that among MO-based nanofluids Fe₃O₄ nanoparticles (sample S6) at a concentration of 0.4% registered a higher average BDV with an enhancement of 45% than other nanoparticles. For EO-based nanofluids, Fe₃O₄ nanoparticles (sample S18) at a concentration of 0.4% registered 52% enhancement in BDV. Similarly, in mixed nanofluids the samples S29 (MO + 75% Fe₃O₄ + 25% TiO₂) and S33 (EO + 75% Fe₃O₄ + 25% TiO₂) registered higher enhancement in BDV as 65% and 69%,

respectively. It is inferred from this enhancement in average BDV of MO, EO and mixed nanofluids, the conductive nanoparticles register higher enhancement percentage than other nanoparticles.

The enhancement in BDV of nanofluids is influenced by type, size, shape, and volume concentration of the nanoparticle. Whereas the similar nanoparticle type and shape and volume concentration, BDV is influenced by size of the nanoparticle, i.e., for smaller size nanoparticle the BDV is

higher and vice-versa for increase in size of the nanoparticle [5]. This is caused by collisions between the polarized nanoparticle surface, liquid molecule and volume concentration of interfaces in the liquid insulation. As a result, size and surface area are crucial for breakdown in liquid insulation. The surface area becomes increasingly crucial as nanoparticles get smaller, which increases the likelihood of charges building up at liquid insulation interfaces.

Many scientists agree that the growth of streamers is responsible for the change or enhancement of the BDV of insulation liquid by the addition of nanoparticles. By acting as electron scavengers, nanoparticles lower the charge density and prevent the growth of streamers in nanofluid, raising the breakdown voltage. The enhancement in BDV of nanofluids by the electron scavenging effect is clearly explained by Peppas [17] and Makmud [18]. This postponed the generation of streamers and slowing down the streamer development process. The BDV of the nanofluids is often influenced by the conductive nanoparticles. According to a paper, conductive nanoparticles swiftly catch fast-moving electrons and change them into slower negatively charged nanoparticles, which slows streamer development and raises breakdown voltage [19]. Our experimental findings confirm that conductive nanoparticle (Fe_3O_4) performs superior than semi-conductive nanoparticles (TiO_2 and ZnO), whereas insulating particles increase BDV quite similarly.

The higher BDV of Fe_3O_4 nanoparticles compared to semi-conductive nanoparticles (TiO_2 and ZnO) is the result of Fe_3O_4 's easier ability to accumulate charges at its surfaces and to become polarized than the other two types of nanoparticles. Conductive nanoparticles entrap moving electrons when an electric field is present; these surface charges are referred to as induced charges. TiO_2 and ZnO nanoparticles, which are nonconductive, trap electrons due to polarization effects. Devins et al. [20] provided a model that they considered the field ionization happens in the liquid to describe how electronic scavenger agents affect streamer propagation. To estimate the amount of positive and negative carriers present in a cylinder-shaped conducting channel, they applied Zener's tunneling theory for solids. This model assumes that the positive streamer speed is constant over the entire electrode gap. While electron injection and trapping are followed by ionization within the liquid in order to propagate negative streamers. It produces plasma that is comparable to that created if the point is in positive. The time taken in either the injection stage or the trapping step determines the negative streamer velocity. If this model needs to be justified for some of its assumptions [20], it is backed by two fascinating facts: (i) Electronic scavengers are added, which reduces the time spent in the trapping distance, first step and increasing the negative velocity. (ii) With the addition of low ionization potential compounds, increase in rate of ionization

shortens the time spent in the second step and enhances the velocity.

When the polarization-relaxation time τ of nanoparticles is subjected to an electric field that can have an impact on the streamer production or not is discussed in [21]. The streamer is suppressed, and the BDV will rise if the τ is lesser than the streamer's growth time. If τ is longer than the streamer's growth time, on the other hand, neither the streamer nor the breakdown voltage will be impacted. This explanation is in conflict with findings related to the impact of electronic scavenger substances including carbon tetrachloride, iodobenzene, and Weibull hexafluoride [22]. It is true that these substances speed up the spread of streamers in liquids.

When nanofluids conduct, nanoparticles may behave as charge carriers' scavengers. If so, they will minimize the amount of charges by trapping, which will in turn diminish the overall space charge. The liquid insulations BDV raises as a result of this decrease in conductivity [18]. The dielectric constant and conductivity of the liquid insulation and nanoparticles influence the improvement in BDV. When these two parameters for nanoparticles and nanofluids are close together, the BDV suffers; however, if these two parameters are dissimilar, the BDV improves.

By acting as electron scavenger at the electrodes and nanofluid interface, nanoparticles play two key roles in enhancing breakdown voltage: (1) increasing the starting voltage of streamers; and (2) forming a double layer at the insulation liquid and nanoparticle interfaces that trap electrons moving within the majority of nanofluid. The effect of electron scavenging stops when the double layers are saturated, which explains why the ideal concentration of nanoparticles produces the highest value of BDV for nanofluids. Due to the enormous volume percentage of interfaces in nanofluid and subsequent linkages between liquid insulations molecular structure and nanoparticles surface, it is noticed that at a given concentration of nanoparticles, the BDV are greater for smaller nanoparticles. As a result, charge carrier motion is delayed, which in turn slows the growth of streamers.

6 Conclusion

In this work, the BDV of MO- & EO-based Fe_3O_4 , ZnO and TiO_2 nanofluids at various concentrations is examined. Moreover, the BDV of mixed nanofluids (i.e., blending of more than one nanoparticle at various concentrations) is also examined. From the results, the conductive nanoparticles blended MO- and EO-based nanofluids reported with highest enhancement percentage in BDV as 45% (sample S6 (MO + 0.4% Fe_3O_4)) and 52% (sample S18 (EO + 0.4% Fe_3O_4)), respectively, compared to other nanoparticles. Among the mixed

nanofluids, the samples S27 (MO + 75% Fe₃O₄ + 75% TiO₂) and S33 (EO + 75% Fe₃O₄ + 25% TiO₂) reported with highest enhancement percentage in BDV as 65% and 69%, respectively. While comparing the BDV of individual nanofluid samples and mixed nanofluid samples, the mixed nanofluid samples have higher enhancement percentage.

Furthermore, Weibull and normal distribution statistical analysis are carried out for examined nanofluids. This depicts that most of the nanofluids follows both Weibull and normal distribution except the samples S5 (MO + 0.3% Fe₃O₄), S10 (MO + 0.4% TiO₂), S13 (MO + 0.3% ZnO), S17 (EO + 0.3% Fe₃O₄), S21 (EO + 0.3% TiO₂), S26 (EO + 0.4% ZnO), S30 (MO + 75% Fe₃O₄ + 25% ZnO) and S36 (EO + 75% Fe₃O₄ + 25% ZnO). One of the major requirements of transformers is higher BDV, and this is fulfilled by these nanofluids. Hence, this may be considered to replace traditional MO in transformers.

Authors' contribution Conceptualization, methodology, experiments and writing were contributed by M. Yamuna.

Conceptualization, methodology, review and editing were contributed by R. Madavan.

Funding There is no funding source available for this research.

Data availability Not applicable.

Declarations

Ethics approval Not applicable.

Consent to participate Not applicable.

Consent to publish Not applicable.

Competing interests The authors declare no competing interests.

References

- Bartnikas R (1994) "Electrical Insulating Liquids," Engineering Dielectrics. ISBN: 9780803120556, Ame Soc Testing Mater 3
- Fofana I (2013) 50 Years in the Development of Insulating Liquids. *IEEE Electr Insul Mag* 29(5):13–25
- Oommen TV (2002) "Vegetable oils for liquid-filled transformers. *IEEE Electr Insul Mag* 18(1):6–11
- Madavan R, Balaraman S (2017) Comparison of Antioxidant Influence on Mineral Oil and Natural Ester Properties under Accelerated Aging Conditions. *IEEE Trans Dielectr Electr Insul* 24(5):2800–2808
- Rengaraj Madavan, Mariappan Ravindran and Subburaj Senthil Kumar (2020) "Evaluating critical characteristics of vegetable oil as a biodegradable insulating oil for transformer". *Int J Emerg Electr Power Syst* 21(5)
- Madavan R, Balaraman S (2017) Investigation on effects of different types of nanoparticles on critical parameters of nano-liquid insulation systems. *J Mol Liq* 230:437–444
- Choi S (1995) Enhancing thermal conductivity of fluids with nanoparticles. *Dev Appl Non-Newtonian Flows ASME FED* 231:99–105
- Segal V, Hjortsberg A, Rabinovich A, Natrass D and Raj K (1998) "AC (60 Hz) and impulse breakdown strength of a colloidal fluid based on transformer oil and magnetite nanoparticles." in Proceedings of the Conference Record of the IEEE International Symposium in Electrical Insulation, 619–622
- Takada T, Hayas e Y, Tanaka Y, Okamoto T (2008) Space charge trapping in electrical potential well caused by permanent and induced dipoles for LDPE/MgO nanocomposite. *IEEE Trans Dielectr Electr Insul* 15(1):152–160
- Yuefan Du, Lv Y, Li C, Chen M, Zhong Y, Zhou J, Li X, Zhou Y (2012) Effect of semiconductive nanoparticles on insulating performances of transformer oil. *IEEE Trans Dielectr Electr Insul* 19(3):770–776
- Yuefan Du, Yuzhen Lv, Chengrong Li, Mutian Chen, Jianquan Zhou, Xiaoxin Li, You Zhou and Youping Tu (2011) "Effect of electron shallow trap on breakdown performance of transformer oil-based nanofluids". *J Appl Phys* 110(10)
- R Madavan, S Senthil Kumar, M Willuice Iruthyarajan (2018) "A comparative investigation on effects of nanoparticles on characteristics of natural esters-based nanofluids" *Colloids Surf. A Physicochem. Eng* 556: 30-36
- Yuan-xiang Z, Yun-shan W, Ji-huan T, Yan-chao S (2010) JIANG Xin-xin, GAO Sheng-you, SUN Qing-hua, and NIE Qiong, "Breakdown characteristics in transformer oil modified by nanoparticles." *High Volt Eng* 36(5):1155–1159
- Yang B, Han ZH (2006) "Temperature-dependent thermal conductivity of nanorod-based nanofluids". *J Appl Phys* 89(8)
- IEC (1995) 60156 International Standard, Insulating liquids - Determination of the breakdown voltage at power frequency - Test method, Second edition
- Shapiro SS, Wilk MB (1965) An analysis of variance test for normality (complete samples). *Biometrika*. 52(3 and 4):591–611
- George D, Mallery M (2010) SPSS for Windows Step by Step: A Simple Guide and Reference. Pearson, Boston
- Peppas G, Charalampakos P, Pyrgioti E (2016) Statistical investigation of AC breakdown voltage of nanofluids compared with mineral and natural ester oils. *IET Sci Meas Technol* 10(6):1–9
- Ibrahim M, Abd-Elhady A, Izzularab M (2016) Effect of nanoparticles on transformer oil breakdown strength: Experiment and theory. *IET Sci Meas Technol* 10:839–845
- Sima W, Shi J, Yang Q et al (2015) Effects of conductivity and permittivity of nanoparticle on transformer oil insulation performance: Experiment and theory. *IEEE Trans Dielectr Electr Insul* 22(1):380–390
- Devins C, Rzad S, Schwabe J (1981) Breakdown and pre-breakdown phenomena in liquids. *J Appl Phys* 52(7):4531–4545
- Hwang J, Zahn M, O'Sullivan E et al (2010) Effects of nanoparticle charging on streamer development in transformer oil-based nanofluids. *J Appl Phys* 107:014310
- Beroual A (1993) Electronic and gaseous processes in the pre-breakdown phenomena of dielectric liquids. *J Appl Phys* 73(9):4528–4533

Publisher's note Springer Nature remains neutral with regard to jurisdictional claims in published maps and institutional affiliations.

Springer Nature or its licensor holds exclusive rights to this article under a publishing agreement with the author(s) or other rightsholder(s); author self-archiving of the accepted manuscript version of this article is solely governed by the terms of such publishing agreement and applicable law.